Estimation of instantaneous peak flows from maximum mean daily flows using the HBV hydrological model

Journal:	*Hydrological Processes*
Manuscript ID	HYP-15-0201.R2
Wiley - Manuscript type:	Research Article
Date Submitted by the Author:	09-Oct-2015
Complete List of Authors:	Ding, Jie; Institute of Water Resources Management, Hydrology and Agricultural Hydraulic Engineering, Leibniz University of Hannover Wallner, Markus; Federal institute for Geosciences and Natural Resources, BGR Müller, Hannes; Institute of Water Resources Management, Hydrology and Agricultural Hydraulic Engineering, Leibniz University of Hannover Haberlandt, Uwe; Institute of Water Resources Management, Hydrology and Agricultural Hydraulic Engineering, Leibniz University of Hannover
Keywords:	model calibration, instantaneous peak flow (IPF), maximum daily flow (MDF), hydrological modeling, rainfall disaggregation model, Aller-Leine catchment, Germany

Estimation of instantaneous peak flows from maximum mean daily flows using the HBV hydrological model

J.Ding[1], M. Wallner[2], H.Müller[1], U. Haberlandt[1]

[1] Institute of Water Resources Management, Hydrology and Agricultural Hydraulic Engineering, University of Hannover, Germany

[2] Federal institute for Geosciences and Natural Resources, Hannover, Germany

Abstract

The record length and quality of instantaneous peak flows (IPFs) have a great influence on flood design, but these high resolution flow data are not always available. The primary aim of this study is to compare different strategies to derive frequency distributions of IPFs using the HBV hydrologic model. The model is operated on a daily and an hourly time step for 18 catchments in the Aller-Leine basin, Germany. Subsequently, General Extreme Value (GEV) distributions are fitted to the simulated annual series of daily and hourly extreme flows. The resulting MDF quantiles from daily simulations are transferred into IPF quantiles using a multiple regression model, which enables a direct comparison with the simulated hourly quantiles. As long climate records with a high temporal resolution are not available, the hourly simulations require a disaggregation of the daily rainfall. Additionally, two calibrations strategies are applied: (a) a calibration on flow statistics; (b) a calibration on hydrographs.

The results show that: (1) the multiple regression model is capable of predicting IPFs with the simulated MDFs; (2) both daily simulations with post-correction of flows and hourly simulations with pre-processing of precipitation enable a reasonable estimation of IPFs; (3) the best results are achieved using disaggregated rainfall for hourly modeling with calibration on flow statistics;

(4) if the IPF observations are not sufficient for model calibration on flow statistics, the transfer of MDFs via multiple regressions is a good alternative for estimating IPFs.

Key words: model calibration; instantaneous peak flow (IPF); maximum mean daily flow (MDF); hydrological modeling; rainfall disaggregation model; Aller-Leine catchment, Germany

1 Introduction

Instantaneous peak flow (IPF) data are the foundation of the design of hydraulic structures and flood frequency analysis. However, long discharge records published by hydrological agencies usually contain only average daily flows which are of little value for design and do not capture the severity of floods, especially in small catchments with little retention.

Given the observed flow data with long enough record lengths, one classical approach to estimating the design IPFs is using a predefined functional relationship of IPF and maximum mean daily flow (MDF) (Fuller 1914, Canuti and Moisello 1982; Fill and Steiner 2003; Langbein 1944; Sangal 1983; Taguas et al. 2008). Based on the development of novel computing technology, several disaggregation algorithms are derived to realize the whole flow series at a finer temporal scale, e.g. from daily to hourly (Stedinger and Vogel 1984; Tarboton et al. 1998; Kumar et al. 2000; Xu et al. 2003; Acharya and Ryu 2014,Dastorani et al. 2013). However, there are a number of difficulties regarding the overall computational and data demand. This may get more difficult as the number of studied basins increase.

In Ding et al. (2014), various statistical methods were presented to estimate the IPFs from MDFs regarding the flood frequency analysis. More precisely, they employed a multiple regression model to construct a functional linear relationship between IPF and MDF at 45 flow stations in

the Aller-Leine basin, Germany. Moreover, the piecewise scaling theory was used to analyze the temporal scaling properties of IPF and MDF data. The subsequent comparison of these methods showed that the multiple regression model has better overall performance. For their investigation eight different probability distributions for extreme values were selected as the candidate distribution. GEV has been proven to be the model of best fit and therefore will be applied in this research.

For investigations concerning the impact of changes in land use, climate and management on runoff extremes, hydrological models have to be used (Cameron et al. 1999; Haberlandt and Radtke 2014). Additionally it might be necessary to estimate IPFs for ungauged sites. In this case, regionalization of hydrological model parameters is commonly applied to transfer information from gauged or partially gauged sites to the target site (Hundecha and Bárdossy 2004; Merz and Blöschl 2004; Oudin et al. 2010; Seibert 1999; Sivapalan 2003; Wallner et al. 2013). Consequently, the IPFs magnitudes and return periods can be estimated by the frequency analysis of flow data generated by a hydrological model with the transferred parameters.

However, the main problem, the lack of long-term observations of high resolution climate data, remains. One possible solution would be to run the hydrological model with stochastically generated high resolution rainfall data (Blazkova and Beven 2004; Cameron et al. 1999; Haberlandt et al. 2008; Haberlandt and Radtke 2014; Viglione et al. 2012). Another alternative would be to run the hydrological model with the longer available daily climate forcing data and then scale the simulated flows or derived extreme values afterwards. It is not known which of the two options provides better results. The main objective of this study is to compare these two alternatives regarding the performance to simulate IPFs using the HBV model.

Considering stochastic rainfall as input, the direct calibration of the hydrological model on observed flow statistics is a good alternative to the standard procedure using the hydrograph for calibration. For the former calibration strategy, additional information in the form of an extreme value distribution and flow duration curve can be used to improve the performance in simulating extremes (Cameron et al. 1999; Haberlandt and Radtke 2014; Westerberg et al. 2011; Yu and Yang 2000).

This study advances previous work using the HBV model by comparing the estimates of IPFs from daily simulations with post-correction of flows and hourly simulations with pre-processing of precipitation, through two different calibration strategies using hydrographs and flow statistics, respectively. The availability of a relatively large number of sites with good, continuous daily data makes it easy to carry out the frequency analysis of the daily extremes. The greatest limitation of frequency analysis based on hourly flow data is the need for climate input data with 1h resolution. Due to increasing computational power this problem has been solved by coupling long, stochastically generated rainfall series with continuous rainfall-runoff simulation (Blazkova and Beven 2009; Faulkner and Wass 2005; Sivapalan et al. 2005). Here, a rainfall disaggregation model, which is a multiplicative random cascade model with exact mass conservation of observed daily data (Müller and Haberlandt 2015; Olsson 1998), is used to provide the hourly rainfall input data. The subsequent frequency analysis of hourly simulation results can then lead to estimations of IPFs with the desired recurrence interval directly.

Which of the above methods is applied to a specific design problem most often depends on the data availability and catchment properties. When determining the appropriate method, one should keep the strength and weaknesses of the different methods in mind. So far there are no studies that have tried to compare these two methods. The aim of this paper therefore is to

provide support for the selection of the best method in estimating IPFs by comparing the daily and hourly simulations combined with two calibration strategies.

The paper is organized as follows: first an introduction to the methodology is provided in the next section followed by a description of the study area and data. Then, the results of different estimation strategies for computing IPFs are discussed. In the final section, the conclusions for this research are described.

2 Method

2.1 Hydrological modeling

2.1.1 HBV model

The applied hydrological model in this study is a version of the HBV model that was originally developed at the Swedish Meteorological and Hydrological Institute (SMHI) in early 1970s (SMHI 2008) and modified by Wallner et al. (2013). It is a simple conceptual and fast running model. It has also been popularly used in several flood simulation studies all over the world (Hlavcova et al. 2005; Velasco et al. 2013). A scheme of the model structure is shown in Figure 1.

Figure 1. Main structure of the HBV model (modified after Killingtveit and Sælthun 1995)

For the purpose of clarity, only the six calibrated parameters are explained in Table 1.These are all conceptual parameters, which are often not easy to estimate from physical catchment properties (Hundecha and Bárdossy 2004; Seibert 1997). The choice of these six calibration

parameters follows a preliminary sensitivity and uncertainty analysis, where the validity for using the same ranges of parameter values on both a daily and an hourly time step has been checked. Further details about the model parameters can be found in Wallner et al. (2013).

Table 1 The calibrated HBV model parameters

2.1.2 Automatic calibration of the hydrological model

The optimization algorithm employed in this study is the dynamically dimensioned search algorithm (DDS), a stochastic, single objective search method that has been proven to be efficient in finding 'good quality' global solutions (see Tolson and Shoemaker (2007)). Compared with other optimization strategies, such as Shuffled Complex Evolution (SCE) and PEST, it has been shown to be able to provide better overall results for the analysis of climate impact on floods in macroscale catchments by Wallner et al. (2012).

Initially, a set of six parameters is selected randomly from the predefined ranges which, are then perturbed by values sampled from a normal distribution. The number of perturbed parameters decreases with an increasing number of iterations such that the solver searches more globally at the beginning and more locally at the end of the optimization process. The DDS algorithm is implemented to calibrate the HBV model in a lumped mode on both a daily and an hourly time step with a total evaluation number of 2000 iterations.

2.2 Precipitation preprocessing using a rainfall disaggregation model

For the calibration of the models, long and high-resolution rainfall time series are necessary. Observed time series of this kind are often too short. On the contrary, time series from non-

recording stations (daily values) exist for much longer periods and with a higher network density. These observed daily values can be potentially disaggregated using information about the time series from nearby recording stations to solve the problem of data scarcity.

For this study a multiplicative random cascade model (Güntner et al. 2001; Olsson 1998) is used for rainfall disaggregation. The rainfall amount of one coarse time step (here daily) is divided into b finer time steps of equal length, where b is the branching number. With b=3 in the first disaggregation step (see Figure 2) a temporal resolution of 8h is achieved. For further disaggregation steps, b=2 is applied, so that temporal resolutions of 4h, 2h and finally 1h are achieved. The applied cascade model is micro-canonical, so the rainfall amount is conserved exactly during the disaggregation procedure for each time step. An aggregation of the disaggregated time series would result in the same time series as before the disaggregation. For a more detailed explanation of the cascade model itself, one can refer to Müller and Haberlandt (2015).

Figure 2. Scheme of the cascade model for rainfall disaggregation

From the peer experiments, we found out the impact of diurnal variation of the evaporation and temperature is not noticeable for the peak flow simulations. The daily temperature values are therefore regarded as constant over the whole day, whereas the daily evaporation values are uniformly divided over 24 hours.

2.3 General procedures to estimate the instantaneous peak flows

The conceptual semi-distributed model HBV is operated on an hourly and a daily time step. Two calibration schemes based on hydrographs and multiple flow statistics are applied. Here, all the available flow data are used for the calibration. A real validation of the hydrological model using a different data period is not feasible because of the short hourly observation period on one hand and the required full peak flow sample for calibration on extreme value statistics on the other hand.

Annual maximum flows (IPF or MDF) are selected from the simulated flow time series. Then, frequency analysis of the extreme values based on the GEV distribution with L-moments (see Hosking and Wallis (1997)) is carried out to estimate certain flood quantiles (T=10, 20, 50, 100yr). The estimated quantiles of IPFs from daily simulations with post-correction of the derived MDF quantiles and hourly simulations with pre-processing of daily observed precipitation are finally compared. Figure 3 gives an overview of the workflow used in this investigation.

Figure 3 Scheme of the two approaches; the temporal resolution of the data is given in brackets

2.3.1 Description of the post-correction approach

For the post-correction approach the hydrological model is operated at a daily time step followed by a subsequent correction of the daily extremes into IPFs. An advantage of this method is the

availability of longer (more than 30 years in our case) observation records based on the denser runoff and climate networks.

The approach consists of three steps:

(1) Calibrate the hydrological model on daily flow statistics (CDF_d) and hydrographs (hydr_d). The direct calibration of the hydrological model on flood distributions (CDF_d) has been proved to have a good performance in many studies for design flood simulation (Cameron et al. 1999; Haberlandt and Radtke 2014). However, the hydrograph calibration strategy is more efficient and applicable regarding the data requirements (Caviedes-Voullieme et al. 2012; Haberlandt and Radtke 2014; Ravazzani et al. 2015).

The objective functions used for both strategies are a combination of Nash-Sutcliffe coefficient (NSC) after Nash and Sutcliffe (1970) for different flow criteria. The determination of weights in the following equations is based on a trial-and-error process to ensure that the hydrological model can give a balanced result for both peak flow simulation and more frequent average flows of hydrograph simulation.

For the calibration against the observed hydrograph (hydr_d) for which the model is forced with observed daily climate data, the objective function is calibrated as:

$$OF_{hydr} = 0.5 \cdot NSC + 0.5 \cdot NSC_{\log} \quad (1)$$

where NSC_{log} is the NSC calibrated with log transformed flows.

For the CDF_d strategy a weighted total Nash-Sutcliffe coefficient (NSC) is computed from the following objective function.

$$OF_{CDF} = 0.275 \cdot NSC_{CDF-SUM} + 0.275 \cdot NSC_{CDF-WIN} + 0.20 \cdot NSC_{FDC} + 0.25 \cdot NSC_{Extremes} \quad (2)$$

where the index CDF is the cumulative distribution function of daily extremes for summer (SUM) (May-October) and winter (WIN) (November-April); FDC is the flow duration curve and Extremes is the annual maximum daily flow series. According to the peer simulation experiments, the sum of weights for summer and winter is set to 55%. The remaining 45% are then portioned between annual maximum daily series and flow duration curve to have a more balanced and robust result.

(2) Select the sample of the annual maximum daily winter/summer flows from the simulations and fit GEV distributions to both samples. Estimate the daily flow quantiles for four different return periods (T=10, 20, 50, 100 yr).

(3) Post correct the MDF quantiles using multiple regression equation that has already been derived in our former research to obtain the IPF from MDF (Ding et al. (2014)):

$$HQ_{IPF} = \alpha_1 \cdot HQ_{MDF} + \alpha_2 \cdot lst\_fp + \alpha_3 \cdot Elv\_ds + \alpha_0 \quad (3)$$

where α_0 … α_3 are regression coefficients; HQ_{MDF} denotes the daily flow quantiles obtained from hydrological simulations and HQ_{IPF} denotes the estimated instantaneous peak flow quantiles; and lst_fp and Elv_ds represent longest flow path and minimum elevation of study basins respectively.

2.3.3 Description of the pre-processing approach

In order to provide a basis for the direct simulation of IPFs, disaggregated daily precipitation has been used because of the restricted availability of observed long continuous rainfall series with high temporal resolution. This method consists of the following steps:

(1) Disaggregate the observed daily precipitation into hourly precipitation. In order to consider the uncertainty in the disaggregation process, 10 realizations of hourly rainfall are generated from historical daily data. This is a compromise between covering the uncertainty and the required computational time.

(2) The calibration of the model with CDF_h strategy is carried out using disaggregated precipitation from the first step and observed flow statistics on an hourly basis of the same time period. The objective function to assess the hourly model performance is Eq. (2) while the Extremes item means here the annual instantaneous peak flow series.

(3) The parameters for hydr_h are derived by calibration of the model on shorter hourly hydrographs using observed hourly rainfall where the objective function is Eq. (1). Then, we transfer the calibrated parameters to the model forced by disaggregated daily rainfall data. The final obtained flood quantiles are the mean value from the 10 GEV distributions fitted to the corresponding 10 optimized disaggregation realizations.

2.3.4 Evaluation of the performance for estimating instantaneous peak flows

The root mean square error (RMSE), bias and Nash-Sutcliffe coefficient (NSC) (Abebe et al. 2010; Nash and Sutcliffe 1970; van Vliet et al. 2012) are the criteria applied for the evaluation of model performance. The RMSE is given by:

$$RMSE = \sqrt{\frac{1}{N}\sum_{i=1}^{N}\left(\frac{HQ_i^* - HQ_i}{HQ_i}\right)^2} \quad (4)$$

The bias criterion is:

$$Bias = \frac{1}{N} \cdot \sum_{i=1}^{N} \left(\frac{HQ_i^* - HQ_i}{HQ_i} \right) \quad (5)$$

where N is the number of stream flow stations; HQ_i^* and HQ_i denote estimated and observed peak flow values respectively.

NSC is computed as:

$$NSC = 1 - \left[\frac{\sum_{i=1}^{n} \left(HQ_i - HQ_i^* \right)^2}{\sum_{i=1}^{n} \left(HQ_i - HQ^{mean} \right)^2} \right] \quad (6)$$

where n is the total number of observations; HQ^{mean} is the mean of the observed peak discharge.

3 Study area and data

The investigations are carried out for 18 catchments within the Aller-Leine river basin in northern Germany (see Figure 4). Their mean elevations rang from 5m.a.s.l (meters above sea level) to 1140m.a.s.l. In the northern part, the river basin is characterized by sandy soils, porous quaternary aquifers and heath and moor vegetation. In the southern part, it is dominated by mountains with largely covered by forests. High annual precipitation and frost are present in the winter season. The sample catchments highlighted in Figure 3 are randomly selected to represent a flat area, a slightly mountainous area and a highly mountainous area, which demonstrate example results in detail for section 4.

The 18 study catchments are located in different geomorphologic and climatologic areas. Table 2 summarizes some of the hydrological characteristics of those catchments. The size of the

catchments is from 45 km^2 to 633 km^2 and the annual precipitation varies between 730 mm/year and around 1500mm/year. The third column in the Table 2 shows the time window of observed discharge as daily flows and monthly peak flow series.

Figure 4. The locations of the 18 catchments of the Aller-Leine river basin in northern Germany

Appropriate processing is performed to establish the distribution of important catchment characteristics based on the GIS digital data. These include a digital elevation model (DEM) with a resolution of 10 meters, a land use map and a river net work. The three characteristics (area, longest flow path and minimum elevation) in Table 2 are derived from the DEM. The portions of the different land use type are derived from the land cover map CORINE2000 (see EUR (1994)). In Figure 4, 17 recording (hourly resolution) and 34 non-recording rainfall stations (daily resolution) are shown. The time series of the recording stations have been used to obtain the parameters for the disaggregation of the daily values. For the determination of area rainfall, time series were interpolated by using the inverse distance method (see Goovaerts, (2000)).

Table 2. List of catchments and their basic descriptors

Records of precipitation with hourly temporal resolution are available for around 6 years from 2003 to 2008 and at a daily time step for the period between 1951 and 2008. The other climate data applied to force the hydrological model, such as temperature and evaporation are available for both temporal resolutions and time periods. Table 3 gives an overview of the time periods of these measurements.

Table 3. Time windows of hydrological data

4 Analysis and results

In this section, first the calibration results of the hydrological model using the observed daily data as input and using the two different calibration strategies (CDF_d and hydr_d) are presented. The multiple regression model is applied to post-correct the simulated MDFs into IPFs. Then the corresponding hourly simulation results by applying disaggregated daily rainfall data (CDF_h and hydr_h) are discussed and finally the performance and uncertainty of the four alternatives are compared for the purpose of estimating IPFs for the 18 catchments.

4.1 Daily simulations with post-correction

4.1.1 Performance of the hydrological model calibrated on flow statistics (CDF_d)

Figure 5 shows comparisons between the fitted probability distributions of daily extremes in winter and summer for the sub-basins Br, De and Pi. These flood frequency results are calculated using observed and simulated daily flow data for over 30 years. The red solid line denotes the fitted GEV distribution on the observed annual daily extremes (black dots). The red dashed lines enclose the 90% confidence interval for the observations obtained by using a bootstrap method after Efron and Tibshirani (1986). The black line corresponds to the simulated distributions, generated using the parameter sets that achieve the best performance for the selected flow statistics. As the small sample size may give rise to uncertain empirical of CDFs for observations, the comparison is then based on the more smooth and robust theoretical CDFs.

It is apparent from Figure 5 that the distribution functions corresponding to the simulated extremes seem to fit the functions derived from observations quite well in winter although there are some deviations in summer for both observed and simulated cases at the higher return periods. In those cases, given the observations only, there could be doubts about the accuracy of

the observed peaks and the ability of the hydrological model to simulate the flow peaks of similar magnitude corresponding to the same storm events that caused the observed peaks. Therefore, more care should be taken for the extrapolation of the fitted distributions in summer as extraordinary extremes appear more often than in winter. One may classify the summer extremes according to their causes.

The uncertainty bands of the observed annual extreme values differ significantly in summer and winter. The wider extent of the confidence interval in summer indicates greater uncertainty than in winter. The Br catchment shows the best fits between the probability distributions derived from the observed and simulated flow peaks in both summer and winter seasons.

Figure 5. Observed and simulated fitted cumulative distribution functions to daily extremes in winter and summer for the three sample catchments (Br/De/Pi); red dashed lines enclose the 90% confidence intervals against observed peak flows

In order to investigate the performance of the hydrological model regarding winter and summer extremes for all 18 catchments, the fitted GEV distributions using observed and simulated extremes are compared. For that a goodness of fit Chi-square test is performed and Figure 6 shows the results in the form of p-values. The red dashed line indicates a 5% significant level. The larger the p-value is, the better the fit. As can be seen, the estimation of winter peaks is far more robust than that of summer peaks with median values (middle black line) in summer and winter of 0.05 and 0.41, respectively. This is consistent with the results obtained above regarding the three sample catchments.

Figure 6. Boxplots of the p-value over 18 catchments comparing the fitted GEV distribution between observed and simulated daily extremes in winter and summer respectively; red dashed line indicates the confidence line (a=0.05)

Figure 7 shows the visual assessments of simulated and observed flow duration curves (FDC) (0.05, 0.25, 0.5, 0.75, 0.95, 0.975 quantiles). One can see that the general fit between simulated (red dashed line) and the observed (blue line) FDC is satisfactory although there are some overestimations in the low flow part of FDCs for the first two catchments. This is likely a result of higher weighting of high flows during the calibration process. In addition, an assessment of FDC fittings for all the 18 catchments is shown in Table 4 with increasing catchment area. The average NSC value is 0.87 with a trend of overestimation suggested by a positive bias value of 20%.

Figure 7. Comparison of observed and simulated daily flow duration curve for the three sample catchments

Table 4. Calibration results of flow duration curve using daily observed precipitation

Figure 8 illustrates the post-correction results using the multiple regression model (Ding et al. 2014) for return periods of 50 and 100 years among the whole study area in winter and summer. IPF (Obs) and IPF (Sim) indicate the quantiles of observed and simulated instantaneous peak

flows respectively. R^2 is the coefficient of determination. Overall, a good agreement between observed and simulated peaks is found. As might be expected, the estimation of the higher return period peaks (T=100yr) is subject to greater estimation errors in both summer and winter season while the estimations in winter are better than in summer.

Figure 8. Comparison between the observed and simulated instantaneous peak flow in winter and summer using the CDF_d strategy at recurrence intervals of 50 and 100 years for all 18 catchments

4.1.2 Performance of the hydrological model calibrated on the daily hydrograph (hydr_d)

Turning to daily hydrograph simulation, it is important to notice that all the observed climate and flow data are used here for calibration. Figure 9 shows only a portion of the calibration results (years 2005 and 2006) at the three sample catchments. It can be seen that, in general, the low flows and the medium peak flows are estimated well although occasional underestimation of the higher peak flows is noticed in De and Pi catchments. Table 5 details the calibration results for all the 18 catchments in the form of their NSC and bias values with increasing catchment area. One can see that good model fits to the observed flow time series are achieved by hydrograph simulation, with NSC value between 0.70 and 0.89 and bias between -1.31% and 5%.

Figure 9. Example of observed and simulated daily hydrographs for the three sample catchments

Table 5. Calibration results for daily hydrographs over the whole record period

Figure 10 shows the post-correction results with respect to the selected MDF series from the hydrograph simulation. The agreement between the observed and simulated IPFs is satisfactory, but with slightly worse estimation results for all the cases compared with Figure 8. Especially, the values of RMSE in winter are higher than the those obtained from the CDF_d strategy.

Figure 10. Comparison between the observed and simulated instantaneous peak flows in winter and summer using the hydr_d strategy at recurrence intervals of 50 and 100 years for all 18 catchments

4.2 Hourly simulations with pre-processing

The results presented in this section are based on continuous hydrological simulations at an hourly time step for the whole observed period. The hydrological model is forced by disaggregated daily to hourly climate data and the obtained results from the two calibration strategies CDF_h and hydr_h are compared with the results from the corresponding daily simulations.

4.2.1 Performance of the hydrological model calibrated on flow statistics (CDF_h)

Figure 11 shows comparisons between the fitted GEV distributions for the three sample catchments in summer and winter season. The red and black solid lines are the results based on observed and simulated annual maxima respectively. The red dashed lines enclose 90% confidence interval of the observed IPFs, represented by black dots. Compared with the corresponding results shown in Figure 5, it is apparent in Figure 11 that the fitted probability distributions from the simulated and observed peaks seem to match fairly well although with a

slight overestimation. Unlike the significant underestimation of flows at higher return periods in summer for daily simulations (see Figure 5), a better agreement between the observed and simulated data fitted to GEV distributions can be seen here at T=100yr. However, it can also be noted that the agreement between the observed and simulated CDFs for lower return periods is a bit poorer than in the corresponding daily simulations. Both the CDF_h and CDF_d strategies are more likely to identify a proper parameter set that reproduces the annual extremes of the observed flow data in winter than in summer.

Figure 11. Observed and simulated fitted CDFs to hourly extremes in winter and summer for the three sample catchments (Br/De/Pi); red dashed lines enclose the 90% confidence intervals against observed peak flows

Figure 12 shows the p-value results in winter and summer from the Chi-square test in which the better "goodness of fit" between simulated and observed IPF distributions for all 18 catchments is indicated by a larger p-value. It can be seen that those results support the findings from above, that the agreement of fitted distributions using observed and simulated peaks is more robust in winter. Additionally, the parameter sets estimated by CDF calibration with hourly hydrologic simulation lead to a better fit between the observed and simulated GEV distribution curves in summer than for the daily simulations (see Figure 6).

Figure 12. Boxplots of the p-values over all catchments for the fitted GEV distribution on observed and simulated hourly extremes in winter and summer; red dashed lines indicate the confidence level of 95% (a=0.05)

A direct comparison of simulated and observed daily FDCs is done by aggregating the hourly simulated flow time series into daily values (Figure 13). Compared with Figure 7, it is apparent that, given the choice of the same target quantiles (0.05, 0.25, 0.5, 0.75, 0.95, 0.975), the aggregated hourly simulations are closer to the observed daily data series in these three sample catchments. The remaining results from the other 14 catchments except Lh shown in Table 6 also agree with it. The poorer estimation performance in Lh can be explained by the pre-processing procedure, as the available daily and hourly rainfall stations involved in the disaggregation are not within the basin (see Figure 4). Given the small sample size for FDC estimation perfect NSC values (NSC=1) result for BP and Ol catchments.

Figure 13. Comparison of observed and simulated daily flow duration curve (FDC) for the three sample basins at an hourly time step

Table 6. Calibration results of flow duration curve (FDC) using the Nash-Sutcliffe criterion (NSC) and the bias criteria

4.2.2 Performance of the hydrological model calibrated on the hydrograph (hydr_h)

Turning to the hourly hydrograph simulation, the visual assessment of the simulation of the three sample catchments is shown in Figure 14. Table 7 details the quantitative assessment for all the 18 catchments. It can be seen that the hydrological model describes the runoff dynamics well with Nash-Sutcliffe values between 0.7 and 0.91 and bias values between -15.5% and 13.62%.

Figure 14. Comparison of observed and simulated hydrographs based on hourly observed precipitation for the three sample catchments

Table 7. Calibration results of continuous hourly hydrograph over the whole record periods

4.3 Comparison between post-correction and pre-processing approaches

Uncertainty is inherent in any flood frequency estimation and results from various sources, such as the statistical techniques applied, the structure and parameters of the hydrological model and the limitations of the observed data.

Figure 15 shows a comparison for the estimation of the 100 yr IPFs including uncertainty bands for the three sample catchments using all of the different methods (CDF_d, CDF_h, hydr_d, hydr_h). In order to consider the error from the hydrological model, 50 parameter sets are optimized for each method to obtain 50 sets of simulated flow peaks. Subsequently, bootstraping is applied to estimate the confidence intervals for the estimated 100 yr IPF with the observed and all sets of simulated flow peaks. For each parameter set, 500 samples of the same length as the calibration period are generated using bootstrapping. This provides 25000 samples for estimation of the uncertainty range for simulated quantiles in this figure. The result based on the observed data series is referred to as OBS, with uncertainty bands based on 500 replications.

The uncertainty bands of OBS in summer are generally wider than in winter for the three sample catchments. Good estimation of IPFs is obtained by calibrating the model on flood frequency curves at both daily and hourly time steps (CDF_d and CDF_h) for which CDF_h gives rise to a larger uncertainty range. The traditional calibration on hydrograph with observed long term daily (hydr_d) and short term hourly rainfall (hydr_h) in general performs poorly. However, the daily

hydrograph simulation (hydr_d) generates smaller uncertainty and better estimation results than the corresponding hourly simulation results (hydr_h). These findings are only proven in the three example catchments.

Figure 15. Estimated 100yr IPFs with 90% confidence bands for the three sample catchments by calibrating the model on flow statistics (CDF_d and CDF_h) and hydrographs (hydr_d and hydr_h) at daily and hourly time steps

Finally, to sum up the contrast between daily simulation with post-correction and hourly simulation with pre-processing over the whole study area for four different return periods (T=10, 20, 50, 100yr) in summer and winter, the RMSE and bias criteria, are estimated to check the overall quality of a given simulation strategy. Figure 16 illustrates the results using daily observed climate data with post-correction and disaggregated daily data with pre-processing to estimate the design IPFs by calibration on flood distributions. Accordingly, the results of Figure 17 are based on calibration using hydrographs.

The first column (MDF-IPF) represents the differences between the observed quantiles of IPFs and the corresponding MDFs without any correction. As can be seen that the immediate replacement of IPF with MDF can lead to significant underestimation with an average RMSE of 30% and bias -30% in winter and 35% and -35% in summer for the four return periods. The estimation from daily calibration with post-correction is shown in the second column (CDF_d). The third column shows the estimation error from calibration at an hourly time step using disaggregated climate data as input (CDF_h).

Figure 17 shows in general that the model calibration at both temporal steps (daily and hourly) is able to effectively predict the IPF. However, using disaggregated daily to hourly rainfall as input provides better overall estimation results with a RMSE of 15 % in winter and 19% in summer although there is a slight underestimation in summer. The accuracy in calibrating the model on daily flow statistics with post correction is similar in summer and winter and the average RMSE is 22% with bias 4%.

Turning to the hydrograph calibration strategy, Figure 17 shows the advantage of the hydr_d approach to estimate the IPFs where observed long-term daily rainfall data as input are combined with subsequent post-correction of daily peaks. This is more notable in the summer season. The RMSE from hydr_d is 25% and 27% for the return periods of 50 yr and 100 yr, respectively, whereas the hydr_h using disaggregated daily precipitation gives 30% for both periods.

Moreover, the bias results show that there is a significant underestimation of IPFs in summer (-18%) and overestimation in winter (10%) when using the disaggregated daily precipitation (hydr_h). The daily simulation with post-correction (hydr_d) produces only a small overestimation for both seasons (6% and 4% respectively).

Figure 16. Comparison of the root mean square error (RMSE) and the bias using the CDF_d and CDF_h strategies for summer and winter seasons

Figure 17. Comparison of the root mean square error (RMSE) and the bias using the hydr_d and hydr_h strategies for summer and winter seasons

5 Conclusions

This research compares two different approaches for the estimation of IPFs, namely, post-correction of the simulated flow data and pre-processing of the daily rainfall input data. Observed daily rainfall and 10 realizations of hourly disaggregated rainfall data are used as input to the rainfall-runoff model HBV. The calibration strategies for model parameter estimation incorporate standard runoff time series calibration (hydr_d and hydr_h) and flow statistics calibration (CDF_d and CDF_h) for 18 catchments in the Aller-Leine river basin, Germany.

In general the final comparison of the results from all 18 catchments suggests the following:

(1) The multiple regression model developed from observed MDFs and IPFs data series is also capable of estimating the IPFs with the modeled MDFs regarding flood frequency analysis.

(2) Generally, the model performances using flow statistics calibration strategy (CDF) are better than those using the traditional hydrograph calibration strategy (hydr) according to the obtained NSC and bias results. The decline in high flow simulation using hydrograph calibration is compensated by an increase in the overall flow simulation. Thus, it shows an advantage to give more balanced simulation results.

(3) The best overall performance for design IPF estimation for all catchments is obtained when disaggregated daily to hourly rainfall data are used for calibration on the observed probability distribution of peak flows (CDF_h). However, the requirement to have observed peak flow data with a long record length fitted to the probability distributions may limit its application in catchments with poor data records.

(4) The daily simulation with post-correction using the same calibration method, namely CDF_d is the second best approach. It has fewer limitations than CDF_h regarding the

length of the observation period of peak flows, as the daily data are more available in most cases. This can help the decision makers and modelers to clarify ideas about how to choose the proper estimation strategy conditioned on available data.

(5) The daily simulation with post-correction (hydr_d) provides better estimation results of IPFs than the corresponding hourly simulation (hydr_h) when the calibration strategy is based on hydrographs. This result demonstrates shorter calibration period (6 years) for hourly simulation would generate worse validation results in terms of the flood frequency analysis compared with the corresponding daily simulation with longer available data (30 years). In general, the hydrograph calibration strategy shows the potential to be used for estimation of design IPFs when the available peak flow data are not long enough to carry out CDF calibration.

Given the computational cost of the simulations, the uncertainty analysis of these two approaches is only carried out for the three sample catchments. The corresponding results in Figure 15 show that the parameter sets obtained from both flood frequency estimation and hydrograph simulation lead to acceptable results. This is consistent with the findings in of Cameron et al. (1999) and Haberlandt and Radtke (2014).

It is important to take uncertainty into account for the robust estimation of instantaneous peak flow using the simulated maximum mean daily flow. However, in this study, we did not cover every aspect of uncertainty, only the final calibration uncertainties are compared. Therefore, one should be aware that the above presented results are case specific regarding the selected hydrological model and calibration methods. It would be beneficial to have more case studies also involving other hydrological models. Further work is under way that considers not only this scaling of the flows but regionalization for unobserved catchments simultaneously.

Acknowledgements

We would like to thank Anna Sikorska, Korbinian Breinl and the other anonymous reviewer for the time and effort they spent on our manuscript. We also sincerely thank for the effort and time Jake Peters has spent as the editor on the manuscript. Special thanks go to Ross Pidoto and Sarah Collins for language editing. We are also grateful for the right to use data from the German National Weather Service (DWD), NLWKN Niedersachsen, Landesamt für Geoinformation und Landentwicklung Niedersachsen, Landesamt für Bergbau and the funding from the China Scholarship Council (CSC).

Reference

Abebe, N.A., Ogden, F.L., and Pradhan, N.R., 2010, Sensitivity and uncertainty analysis of the conceptual HBV rainfall-runoff model: Implications for parameter estimation: Journal of Hydrology, v. 389, p. 301-310.

Acharya, A., and Ryu, J., 2014, Simple Method for Streamflow Disaggregation: Journal of Hydrologic Engineering, v. 19, p. 509-519.

Blazkova, S., and Beven, K., 2004, Flood frequency estimation by continuous simulation of subcatchment rainfalls and discharges with the aim of improving dam safety assessment in a large basin in the Czech Republic: Journal of Hydrology, v. 292, p. 153-172.

Blazkova, S., and Beven, K., 2009, A limits of acceptability approach to model evaluation and uncertainty estimation in flood frequency estimation by continuous simulation: Skalka catchment, Czech Republic: Water Resources Research, v. 45, p. W00B16.

Cameron, D.S., Beven, K.J., Tawn, J., Blazkova, S., and Naden, P., 1999, Flood frequency estimation by continuous simulation for a gauged upland catchment (with uncertainty): Journal of Hydrology, v. 219, p. 169-187.

Canuti, P., and Moisello, U., 1982, Relationship between the yearly maxima of peak and daily discharge for some basins in Tuscany: J. Hydrol.Sci, v. 27, p. 111–128.

Caviedes-Voullieme, D., Garcia-Navarro, P., and Murillo, J., 2012, Influence of mesh structure on 2D full shallow water equations and SCS Curve Number simulation of rainfall/runoff events: Journal of Hydrology, v. 448, p. 39-59.

Dastorani, M.T., Koochi, J.S., Darani, H.S., Talebi, A., and Rahimian, M.H., 2013, River instantaneous peak flow estimation using daily flow data and machine-learning-based models: Journal of Hydroinformatics, v. 15, p. 1089–1098.

Ding, J., Haberlandt, U., and Dietrich, J., 2014, Estimation of the instantaneous peak flow from maximum daily flow: a comparison of three methods: Hydrology Research (in press) doi:10.2166/nh.2014.085.

Efron, B., and Tibshirani, R., 1986, Bootstrap Methods for Standard Errors, Confidence Intervals, and Other Measures of Statistical Accuracy: Statistical Science, v. 1, p. 54-75.

EUR, 1994, EUR 12585 - CORINE land cover project - Technical guide. European Commission. Office for Official Publications of the European Communities. Luxembourg.

Faulkner, D., and Wass, P., 2005, FLOOD ESTIMATION BY CONTINUOUS SIMULATION IN THE DON CATCHMENT, SOUTH YORKSHIRE, UK: Water and Environment Journal, v. 19, p. 78-84.

Fill, H., and Steiner, A., 2003, Estimating Instantaneous Peak Flow from Mean Daily Flow Data: Journal of Hydrologic Engineering, v. 8, p. 365-369.

Fuller, W.E., 1914, Flood Flows: American Society of Civil Engineers, v. 77, p. 564-617.

Güntner, A., Olsson, J., Calver, A., and Gannon, B., 2001, Cascade-based disaggregation of continuous rainfall time series: the influence of climate: Hydrol. Earth Syst. Sci., v. 5, p. 145-164.

Haberlandt, U., Ebner von Eschenbach, A.D., and Buchwald, I., 2008, A space-time hybrid hourly rainfall model for derived flood frequency analysis: Hydrol. Earth Syst. Sci., v. 12, p. 1353-1367.

Haberlandt, U., and Radtke, I., 2014, Hydrological model calibration for derived flood frequency analysis using stochastic rainfall and probability distributions of peak flows: Hydrol. Earth Syst. Sci., v. 18, p. 353-365.

Hlavcova, K., Kohnova, S., Kubes, R., Szolgay, J., and Zvolensky, M., 2005, An empirical method for estimating future flood risks for flood warnings: Hydrology and Earth System Sciences, v. 9, p. 431-448.

Hosking, J.R.M., and Wallis, J.R., 1997, Regional frequency analysis:an approach based on L-moments: Cambridge University Press ,New York, USA.

Hundecha, Y., and Bárdossy, A., 2004, Modeling of the effect of land use changes on the runoff generation of a river basin through parameter regionalization of a watershed model: Journal of Hydrology, v. 292, p. 281-295.

Killingtveit, Å., and Sælthun, N.R., 1995, Hydrology: Hydropower Development,v.7, Trondheim, Norway: Norwegian Institute of Technology, Division of Hydraulic
Engineering.

Kumar, D.N., Lall, U., and Petersen, M.R., 2000, Multisite disaggregation of monthly to daily streamflow: Water Resources Research, v. 36, p. 1823-1833.

Langbein, W.b., 1944, Peak discharge from daily records: US Geological survay Bulletin August, v. p.145.

Merz, R., and Blöschl, G., 2004, Regionalisation of catchment model parameters: Journal of Hydrology, v. 287, p. 95-123.

Müller, H., and Haberlandt, U., 2015, Temporal rainfall disaggregation with a cascade model: from single-station disaggregation to spatial rainfall: J. Hydrol. Eng (in press).

Nash, J.E., and Sutcliffe, J.V., 1970, River flow forecasting through conceptual models part I — A discussion of principles: Journal of Hydrology, v. 10, p. 282-290.

Olsson, J., 1998, Evaluation of a scaling cascade model for temporal rain- fall disaggregation: Hydrol. Earth Syst. Sci., v. 2, p. 19-30.

Oudin, L., Kay, A., Andréassian, V., and Perrin, C., 2010, Are seemingly physically similar catchments truly hydrologically similar?: Water Resources Research, v. 46, p. W11558.

Ravazzani, G., Bocchiola, D., Groppelli, B., Soncini, A., Rulli, M.C., Colombo, F., Mancini, M., and Rosso, R., 2015, Continuous streamflow simulation for index flood estimation in an Alpine basin of northern Italy: Hydrological Sciences Journal-Journal Des Sciences Hydrologiques, v. 60, p. 1013-1025.

Sangal, B., 1983, Practical Method of Estimating Peak Flow: Journal of Hydraulic Engineering, v. 109, p. 549-563.

Seibert, J., 1997, Estimation of parameter uncertainty in the HBV model: Nordic Hydrology, v. 28, p. 247-262.

Seibert, J., 1999, Regionalisation of parameters for a conceptual rainfall-runoff model: Agricultural and Forest Meteorology, v. 98–99, p. 279-293.

Sivapalan, M., 2003, Prediction in ungauged basins: a grand challenge for theoretical hydrology: Hydrological Processes, v. 17, p. 3163-3170.

Sivapalan, M., Blöschl, G., Merz, R., and Gutknecht, D., 2005, Linking flood frequency to long-term water balance: Incorporating effects of seasonality: Water Resources Research, v. 41, p. W06012.

SMHI, 2008, Integrated Hydrological Modelling System - Manual Version 6.0,
Swedish Meteorological and Hydrological Institute.

Stedinger, J.R., and Vogel, R.M., 1984, Disaggregation Procedures for Generating Serially Correlated Flow Vectors: Water Resources Research, v. 20, p. 47-56.

Taguas, E.V., Ayuso, J.L., Pena, A., Yuan, Y., Sanchez, M.C., Giraldez, J.V., and Pérez, R., 2008, Testing the relationship between instantaneous peak flow and mean daily flow in a Mediterranean Area Southeast Spain: CATENA, v. 75, p. 129-137.

Tarboton, D.G., Sharma, A., and Lall, U., 1998, Disaggregation procedures for stochastic hydrology based on nonparametric density estimation: Water Resources Research, v. 34, p. 107-119.

Tolson, B.A., and Shoemaker, C.A., 2007, Dynamically dimensioned search algorithm for computationally efficient watershed model calibration: Water Resources Research, v. 43, p. W01413.

van Vliet, M.T.H., Yearsley, J.R., Franssen, W.H.P., Ludwig, F., Haddeland, I., Lettenmaier, D.P., and Kabat, P., 2012, Coupled daily streamflow and water temperature modelling in large river basins: Hydrology and Earth System Sciences, v. 16, p. 4303-4321.

Velasco, M., Versini, P.A., Cabello, A., and Barrera-Escoda, A., 2013, Assessment of flash floods taking into account climate change scenarios in the Llobregat River basin: Natural Hazards and Earth System Sciences, v. 13, p. 3145-3156.

Viglione, A., Castellarin, A., Rogger, M., Merz, R., and Blöschl, G., 2012, Extreme rainstorms: Comparing regional envelope curves to stochastically generated events: Water Resources Research, v. 48, p. W01509.

Wallner, M., Haberlandt, U., and Dietrich, J., 2012, Evaluation of different calibration strategies for large scale continuous hydrological modelling: Adv. Geosci., v. 31, p. 67-74.

Wallner, M., Haberlandt, U., and Dietrich, J., 2013, A one-step similarity approach for the regionalization of hydrological model parameters based on Self-Organizing Maps: Journal of Hydrology, v. 494, p. 59-71.

Westerberg, I.K., Guerrero, J.L., Younger, P.M., Beven, K.J., Seibert, J., Halldin, S., Freer, J.E., and Xu, C.Y., 2011, Calibration of hydrological models using flow-duration curves: Hydrol. Earth Syst. Sci., v. 15, p. 2205-2227.

Xu, Z., Schumann, A., and Li, J., 2003, Markov cross-correlation pulse model for daily streamflow generation at multiple sites: Advances in Water Resources, v. 26, p. 325-335.

Yu, P.S., and Yang, T.C., 2000, Using synthetic flow duration curves for rainfall–runoff model calibration at ungauged sites: Hydrological Processes, v. 14, p. 117-133.

Table 1 The calibrated HBV model parameters

Optimized HBV model parameters	Description and unit	Prior range
tt	threshold temperature for snowmelt [°C]	-2 — 2
fc	the maximum soil moisture storage [mm]	30 — 600
β	a shape coefficient [-]	0.5 — 8.0
Hl	a threshold value of water content in the upper reservoir [mm]	1 — 30
k0	the storage coefficient of the surface runoff [d]/[h]	0.25 — 5.00
K_{Perc}	storage coefficient of the percolation [d]/[h]	3 — 50

Table 2. List of catchments and their basic descriptors

Nr	basin name	observed flow record	annual precipitation	Area	Longest flow path	Min elevation	urban	agricultural	forest
(-)	(-)	(year)	(mm/year)	(Km^2)	(m)	(m)	(%)	(%)	(%)
1	BS	1968--2007	840.16	127	19689	96.8	4.81	67.99	27.37
2	BP	1967--2007	733.9	116	25747	67.5	6.33	87.58	6.26
3	Br	1962--2007	872.32	285	41802	41.0	4.7	42.75	51.91
4	Go	1959--2006	791.61	633	62868	141.5	7.03	66.95	26.04
5	Gr	1962--2006	1004.74	125	23915	129.4	7.91	48.85	43.22
6	Ha	1974--2007	838.62	104	25244	74.8	6.71	55.5	37.98
7	Ku	1962--2006	910.93	61.8	13524	130.2	1.97	70.39	27.73
8	Lh	1955--2007	854.3	100	25987	24.8	0.94	57.51	41.8
9	Ma	1964--2006	835.91	45	12035	196.2	0.98	67.63	31.49
10	Mt	1967--2007	748.98	242	36744	36.6	28.1	54.34	16.7
11	NP	1967--2006	737.17	334	40583	55.5	3.46	62.01	34.44
12	Ol	1962--2006	1004.16	149	25339	128.6	1.7	31.8	66.43
13	Pi	1952--2006	1537.94	44.5	17112	339.6	0.51	0.24	99.1
14	Re	1964--2006	793.69	321	43413	182.9	5.29	66.09	28.64
15	RH	1962--2006	781.71	184	24915	154.7	6.9	72.46	20.8
16	VR	1964--2006	1136.36	57.5	22158	133.1	15.88	19.19	65.18
17	De	1978--2007	899.57	309	49067	90.9	5.63	56.25	38.08
18	Me	1962--2007	889.15	136	27856	81.9	6.38	58.37	35.28

Table 3. Time windows of hydrological data

Variable	Daily	Hourly
Runoff	29-44 yr	2004-2008
Monthly peak flow	(-)	29-44 yr
Precipitation	1951-2008	2003-2008
Temperature	1951-2008	2003-2008
Evaporation	1951-2008	2003-2008

Table 4. Calibration results of flow duration curve (FDC) using daily observed precipitation

FDCs	Pi	Ma	VR	Ku	Lh	Ha	BP	Gr	BS	Me	Ol	RH	Mt	Br	De	Re	NP	Go
NSC [-]	0.93	0.94	0.94	0.95	0.6	0.91	0.93	0.91	0.89	0.98	0.98	0.74	0.95	0.91	0.92	0.94	0.96	0.96
Bias [%]	-12.07	42.07	62.29	23.25	41.16	27.99	32.44	52.33	59.75	29.81	18.57	85.72	9.23	24.53	35.93	33.11	37.74	15.12

Table 5. Calibration results of continuous daily hydrograph over the whole record periods

hydr_d	Pi	Ma	VR	Ku	Lh	Ha	BP	Gr	BS	Me	Ol	RH	Mt	Br	De	Re	NP	Go
NSC [-]	0.82	0.73	0.7	0.75	0.71	0.8	0.75	0.79	0.76	0.81	0.83	0.74	0.81	0.8	0.85	0.82	0.74	0.89
Bias[%]	-1.31	5.07	4.52	3.15	-0.55	1.18	5	-0.25	5	-0.8	0.34	-0.27	-1.11	-0.56	1.77	0.44	-1.9	-0.84

Table 6. Calibration results of flow duration curve (FDC) using the Nash-Sutcliffe criterion (NSC) and the bias criteria

FDCs	Pi	Ma	VR	Ku	Lh	Ha	BP	Gr	BS	Me	Ol	RH	Mt	Br	De	Re	NP	Go
NSC [-]	0.97	0.81	0.92	0.94	0.51	0.96	1	0.99	0.95	0.89	1	0.94	0.98	0.97	0.96	0.97	0.98	0.99
Bias [%]	-11.43	-5.83	33.31	61.76	32.82	53.21	0.31	6.87	26.5	30.61	2.57	20.95	-13.23	12.78	-12.21	5.19	0.79	-4.88

Table 7. Calibration results of continuous hourly hydrograph over the whole record periods

hydr_h	Pi	Ma	VR	Ku	Lh	Ha	BP	Gr	BS	Me	Ol	RH	Mt	Br	De	Re	NP	Go
NSC [-]	0.85	0.72	0.72	0.75	0.7	0.84	0.75	0.8	0.82	0.74	0.91	0.73	0.81	0.82	0.82	0.78	0.85	0.84
Bias[%]	-15.5	-2.66	-1.22	-7.75	0.6	3.71	13.62	12.3	7.83	-5.67	3.29	2.14	0.09	-0.41	4.2	-2.9	2.98	-0.61

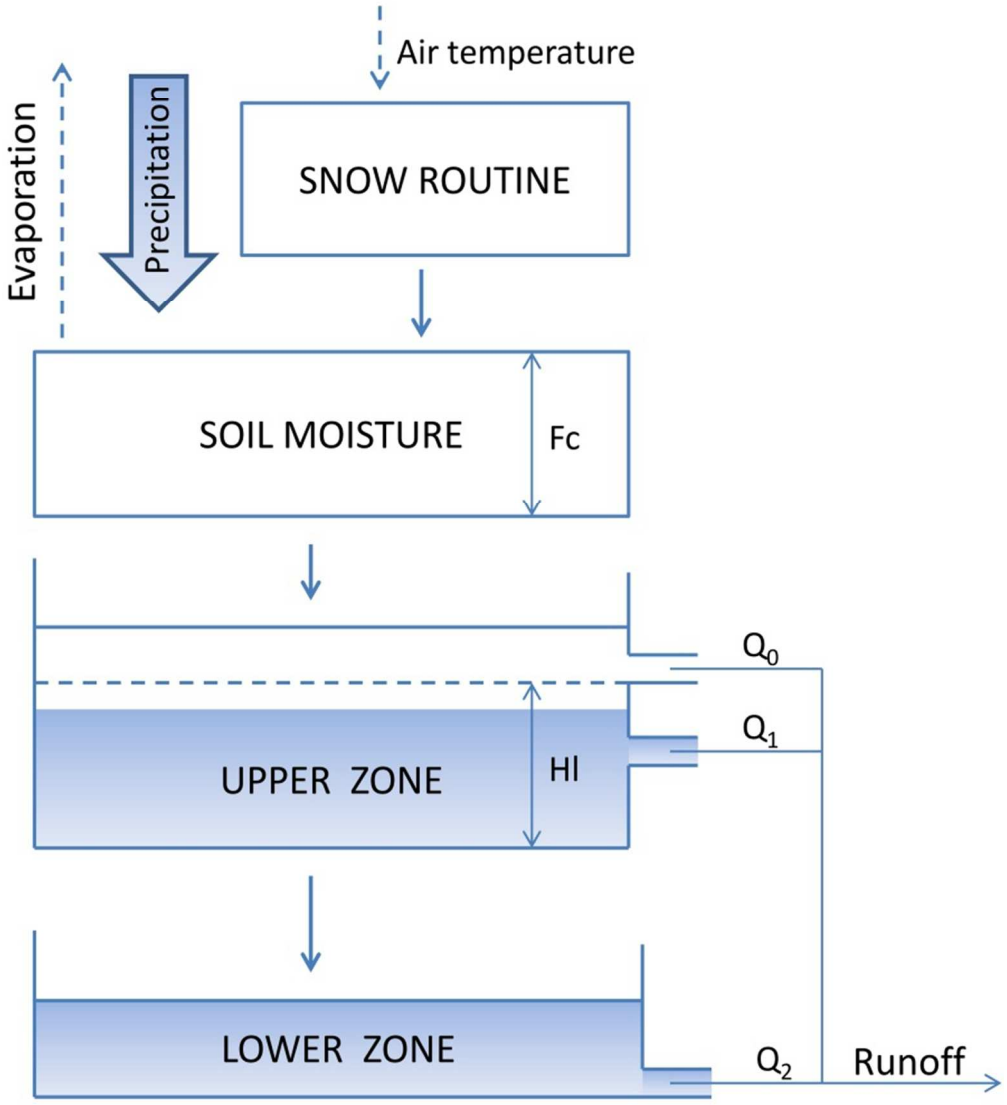

Figure 1. Main structure of the HBV model (modified after Killingtveit and Sælthun 1995)
103x114mm (220 x 220 DPI)

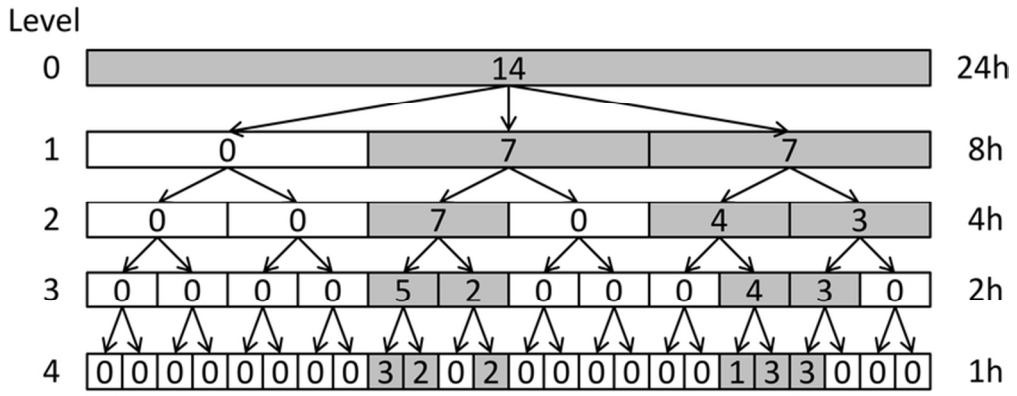

Figure 2. Scheme of the cascade model for rainfall disaggregation
71x27mm (300 x 300 DPI)

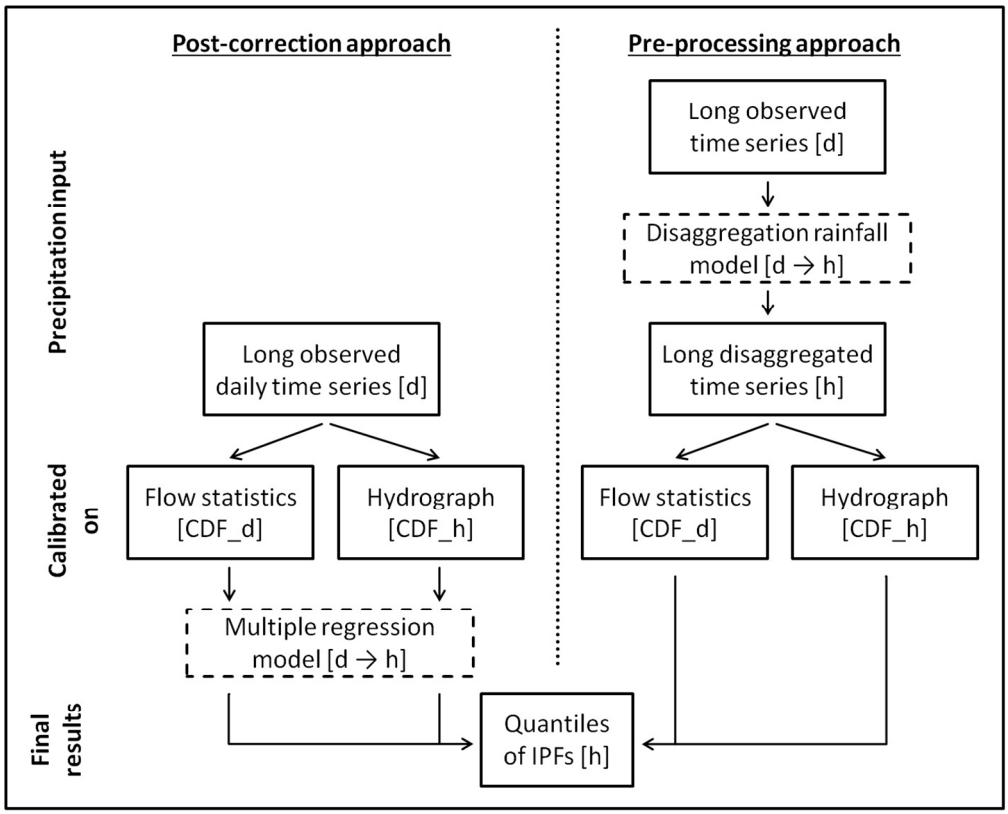

Figure 3。Scheme of the two approaches; the temporal resolution of the data is given in brackets
372x299mm (96 x 96 DPI)

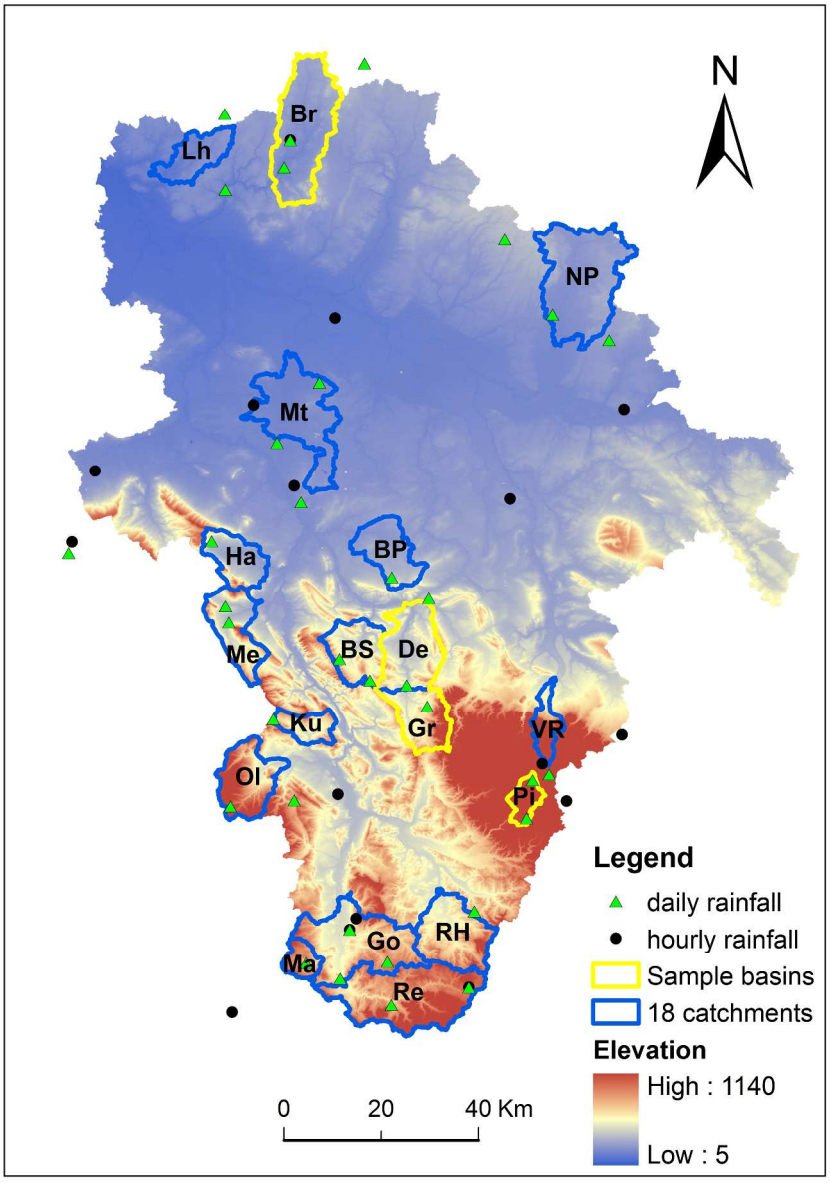

Figure 4. The locations of the 18 catchments of the Aller-Leine river basin in northern Germany
297x420mm (300 x 300 DPI)

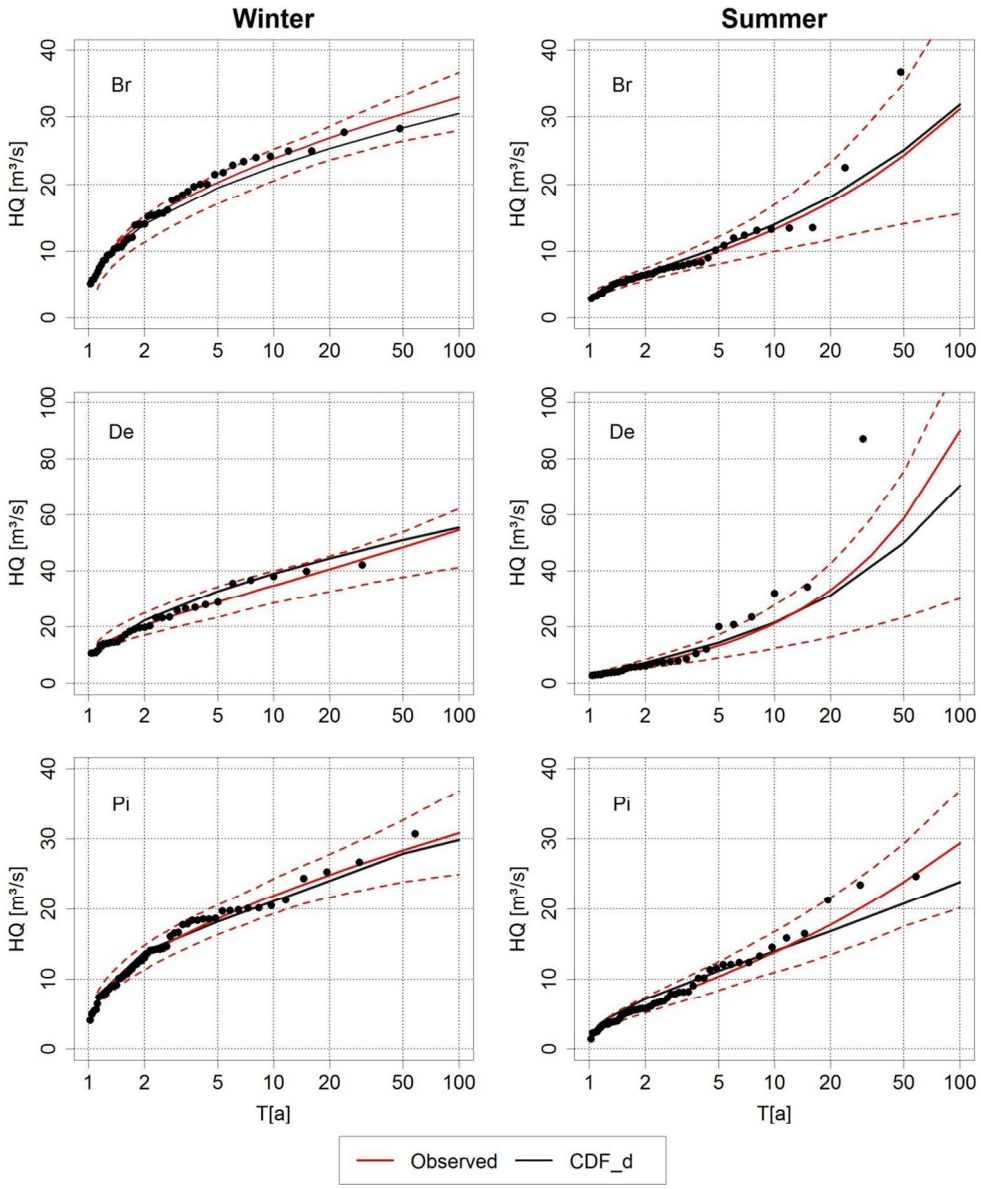

Figure 5. Observed and simulated fitted cumulative distribution functions to daily extremes in winter and summer for the three sample catchments (Br/De/Pi); red dashed lines enclose the 90% confidence intervals against observed peak flows
165x198mm (220 x 220 DPI)

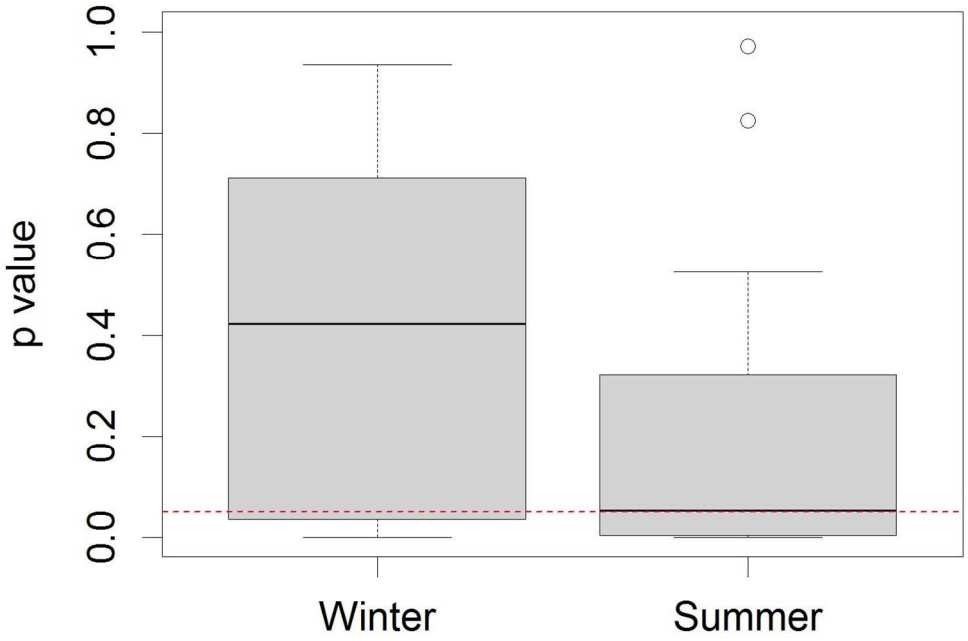

Figure 6. Boxplots of the p-value over 18 catchments comparing the fitted GEV distribution between observed and simulated daily extremes in winter and summer respectively; red dashed line indicates the confidence line (a=0.05)
396x264mm (96 x 96 DPI)

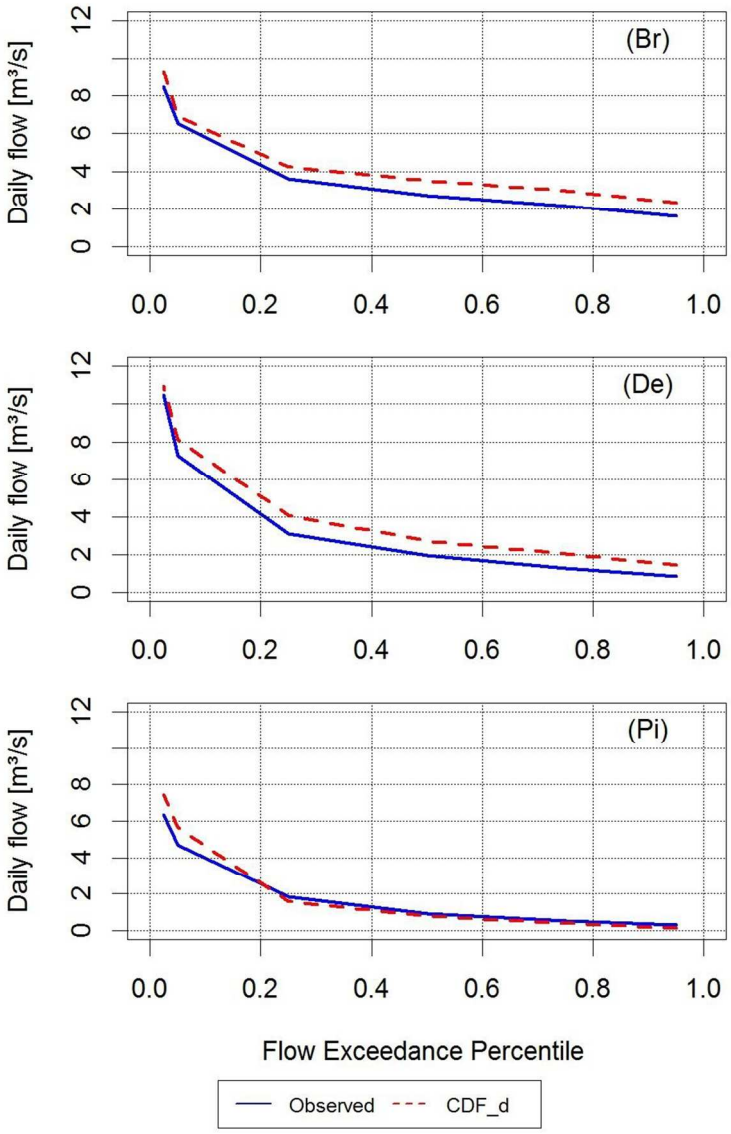

Figure 7. Comparison of observed and simulated daily flow duration curve for the three sample catchments
264x396mm (96 x 96 DPI)

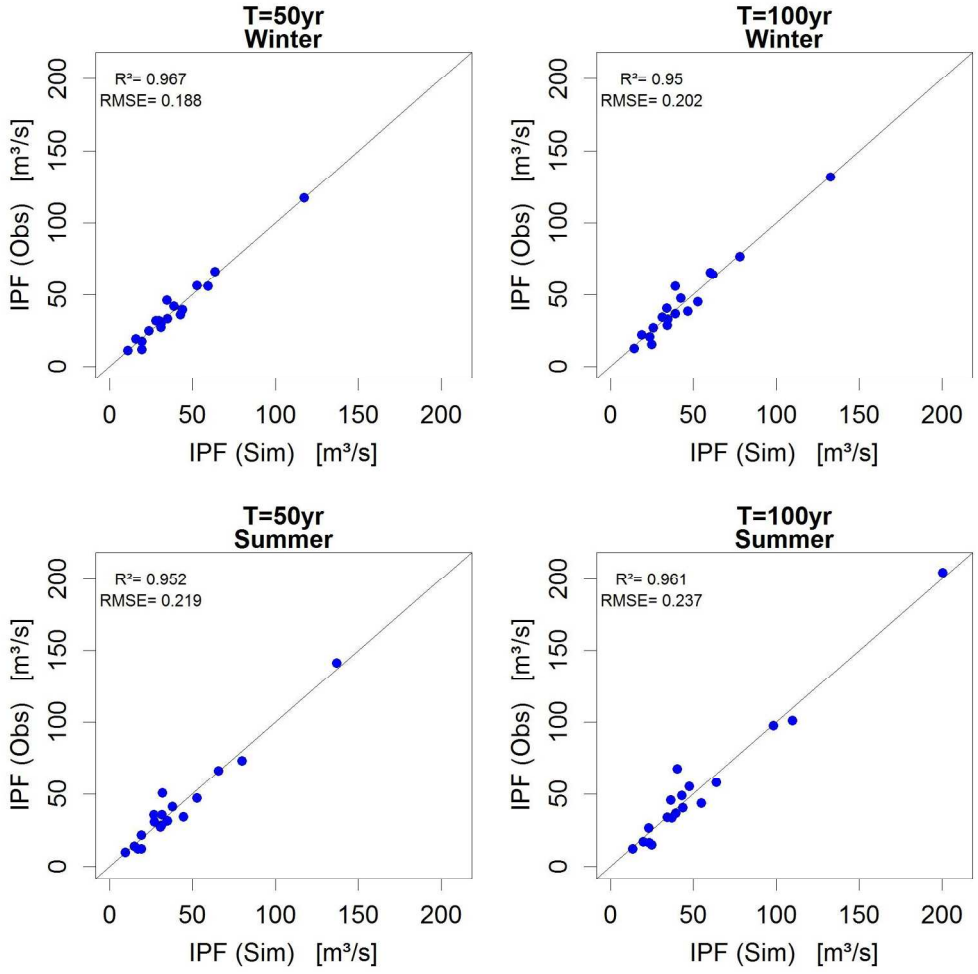

Figure 8. Comparison between the observed and simulated instantaneous peak flow in winter and summer using the CDF_d strategy at recurrence intervals of 50 and 100 years for all 18 catchments
529x529mm (96 x 96 DPI)

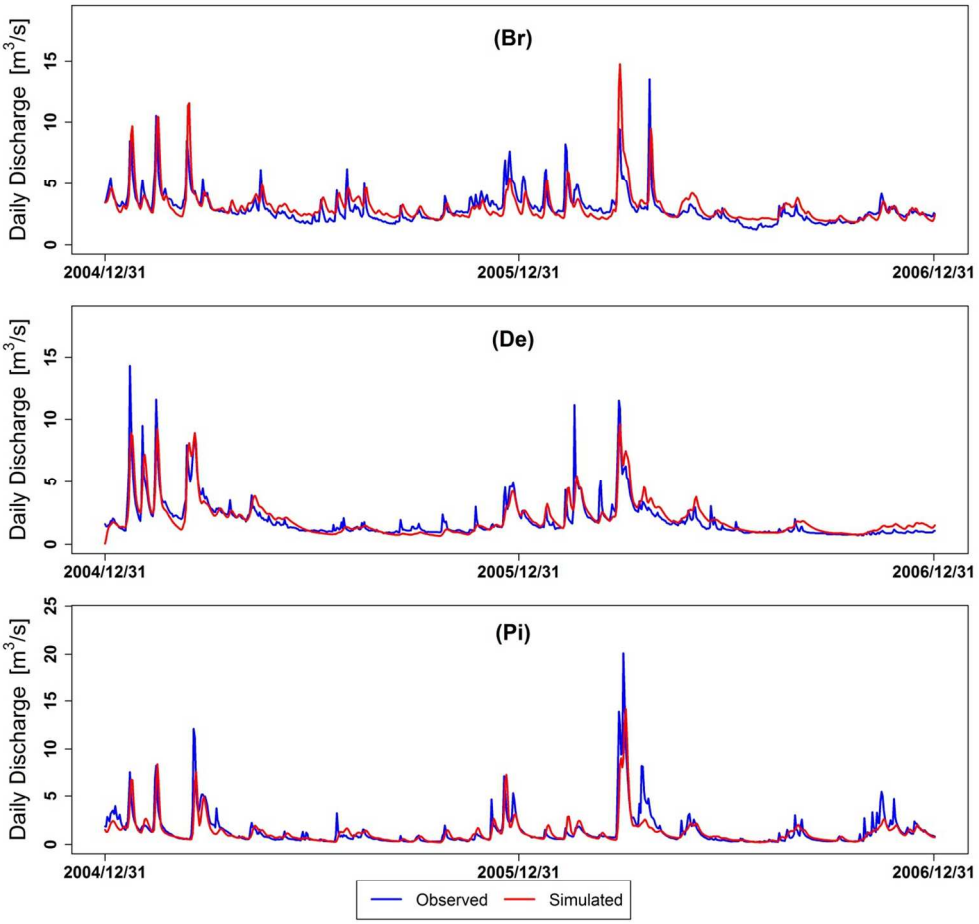

Figure 9. Example of observed and simulated daily hydrographs for the three sample catchments
165x165mm (220 x 220 DPI)

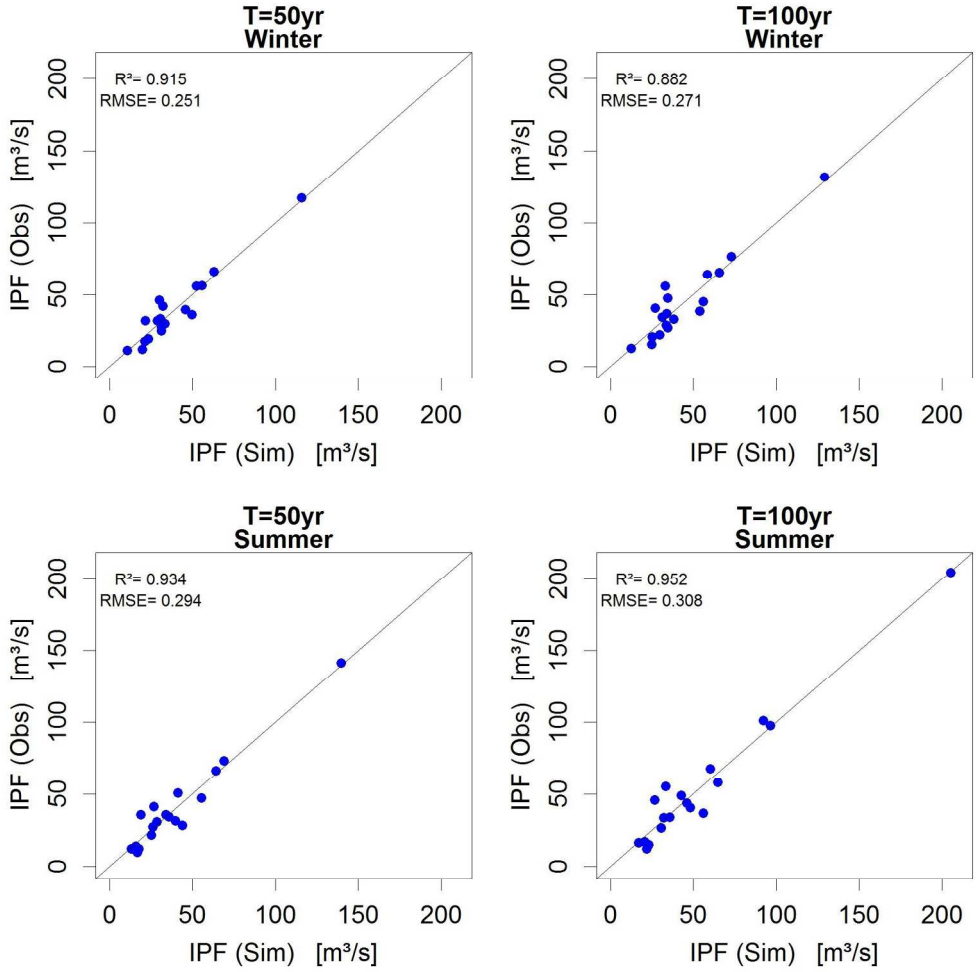

Figure 10. Comparison between the observed and simulated instantaneous peak flows in winter and summer using the hydr_d strategy at recurrence intervals of 50 and 100 years for all 18 catchments
529x529mm (96 x 96 DPI)

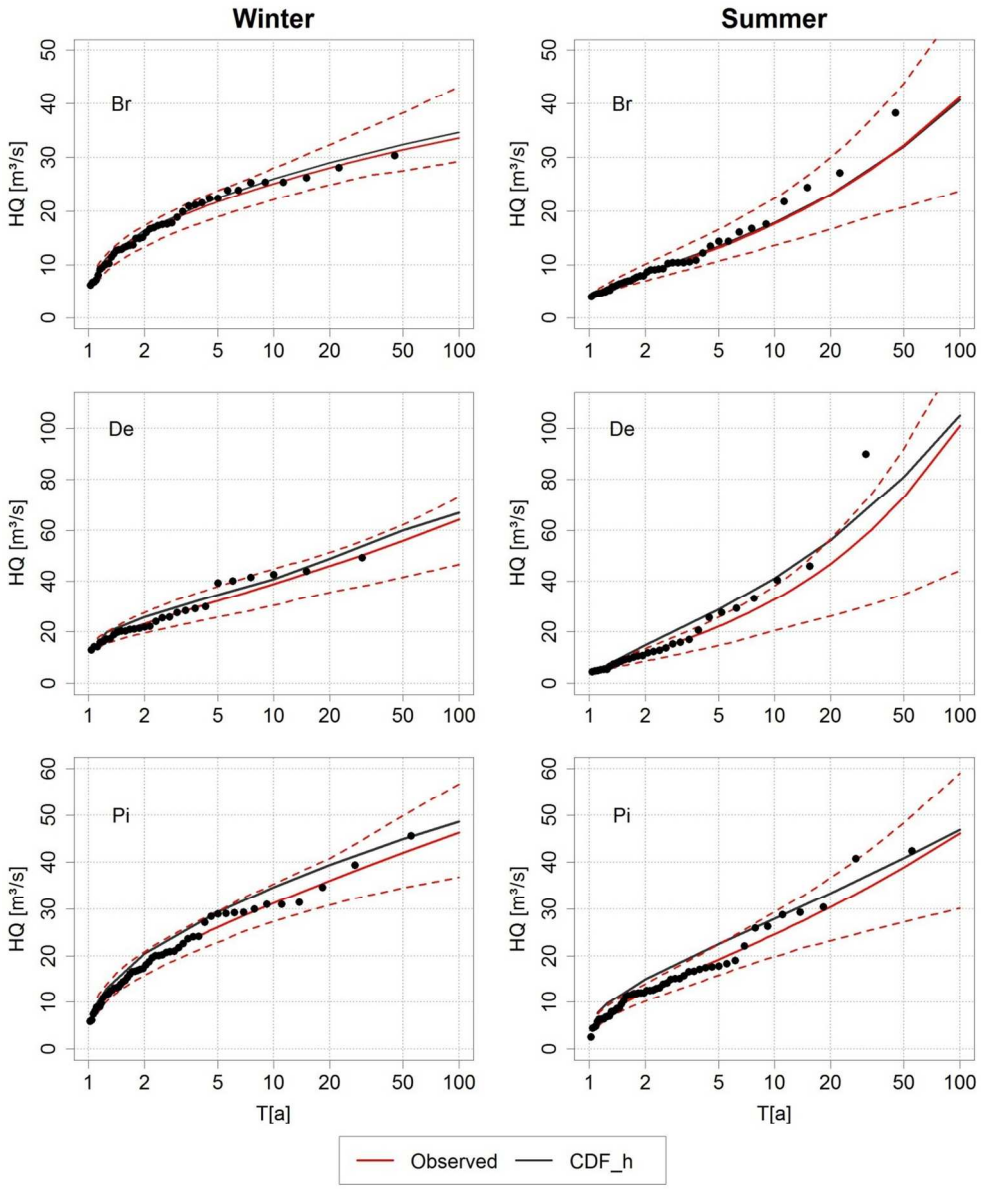

Figure 11. Observed and simulated fitted CDFs to hourly extremes in winter and summer for the three sample catchments (Br/De/Pi); red dashed lines enclose the 90% confidence intervals against observed peak flows
165x198mm (220 x 220 DPI)

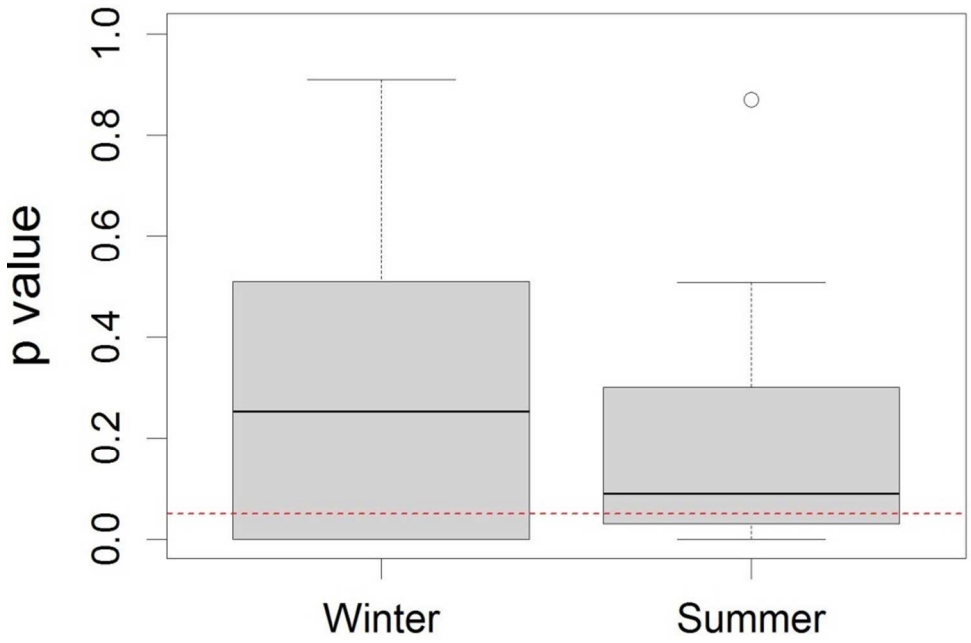

Figure 12. Boxplots of the p-values over all sub-catchments for the fitted GEV distribution on observed and simulated hourly extremes in winter and summer; red dashed lines indicate the confidence level of 95% (a=0.05)
122x81mm (220 x 220 DPI)

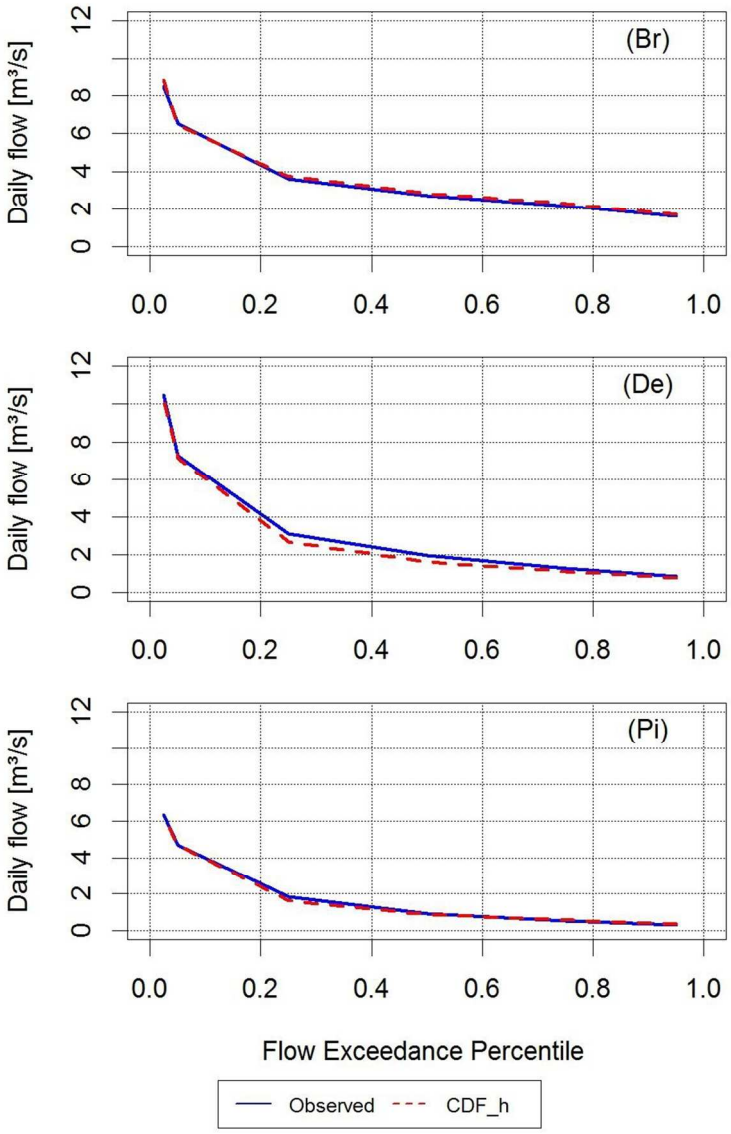

Figure 13. Comparison of observed and simulated daily flow duration curve (FDC) for the three sample basins at an hourly time step
264x396mm (96 x 96 DPI)

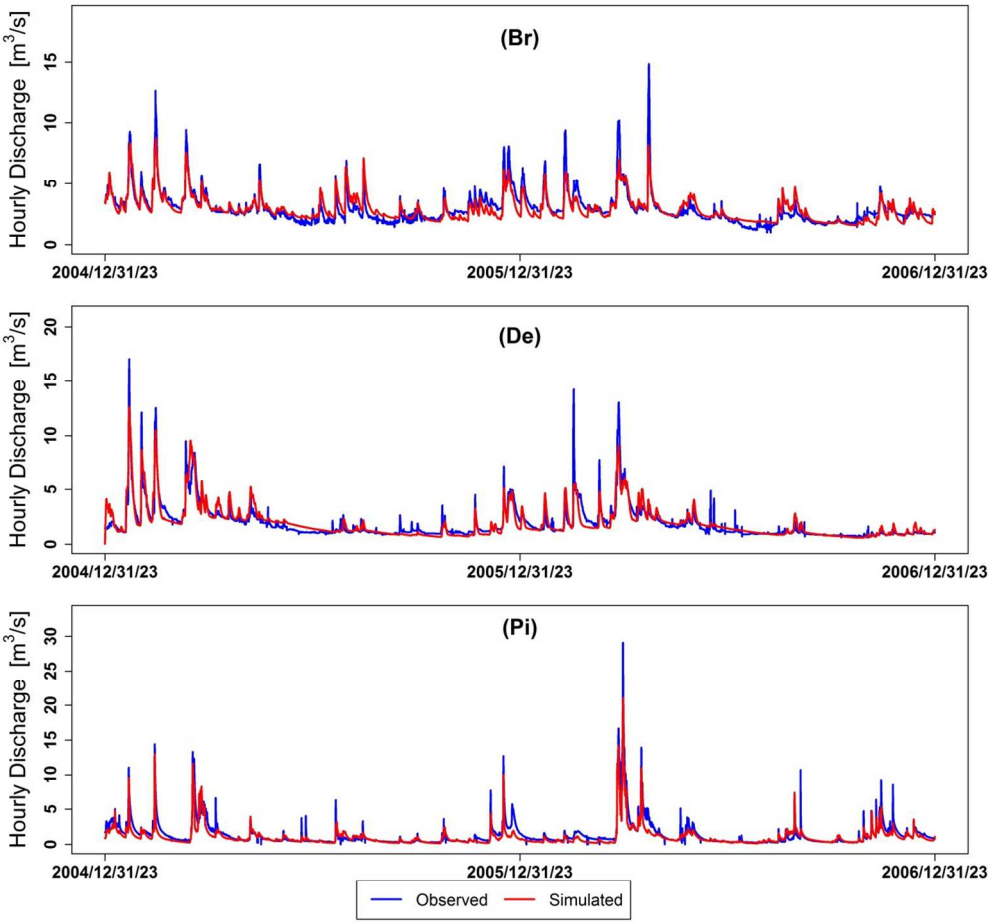

Figure 14. Comparison of observed and simulated hydrographs based on hourly observed precipitation for the three sample catchments
165x165mm (220 x 220 DPI)

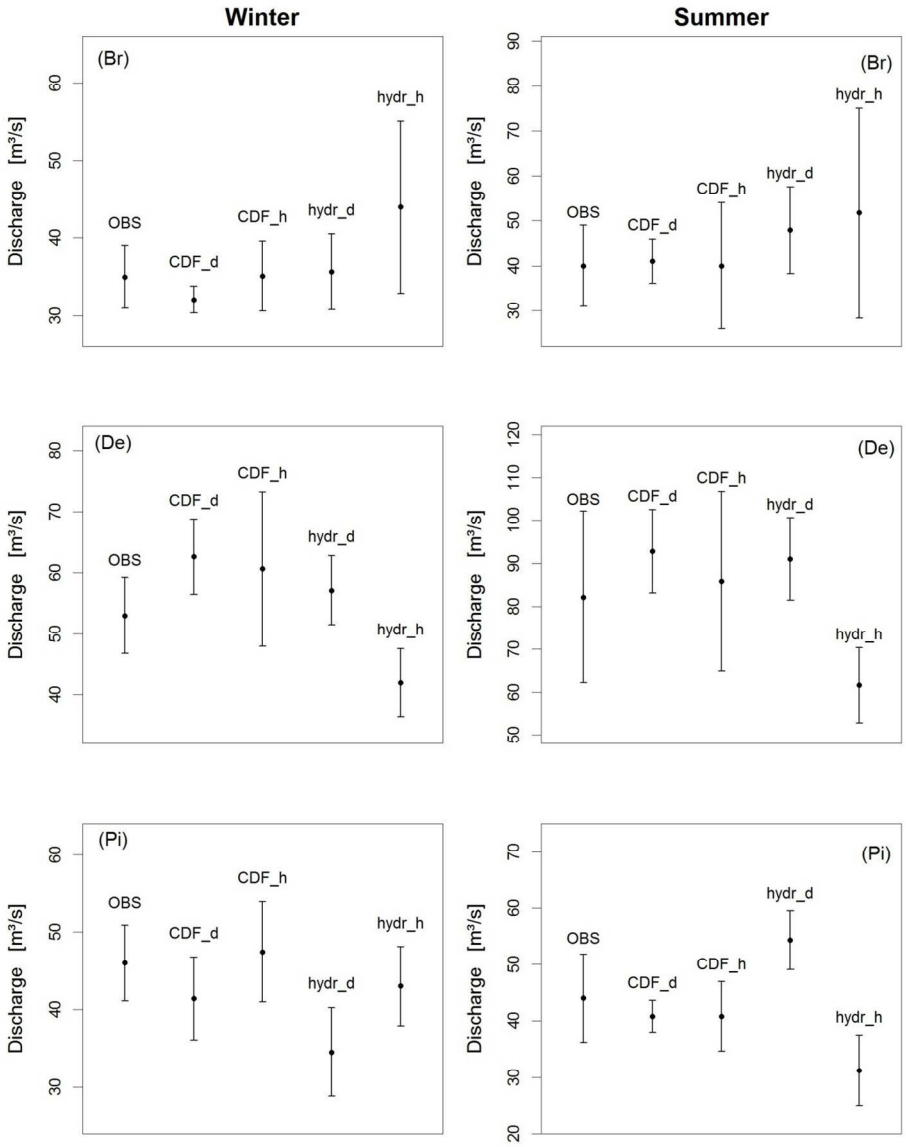

Figure 15. Estimated 100yr IPFs with 90% confidence bands for the three sample catchments by calibrating the model on flow statistics (CDF_d and CDF_h) and hydrographs (hydr_d and hydr_h) at daily and hourly time steps
165x206mm (220 x 220 DPI)

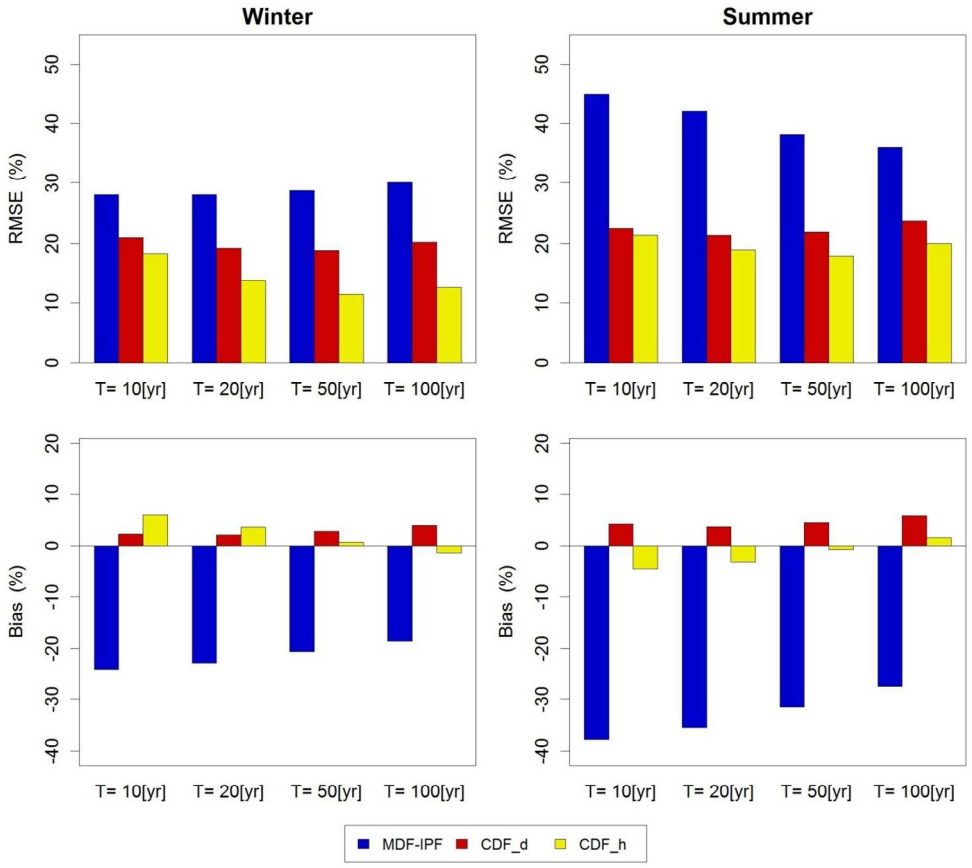

Figure 16. Comparison of the root mean square error (RMSE) and the bias using the CDF_d and CDF_h strategies for summer and winter seasons
165x150mm (220 x 220 DPI)

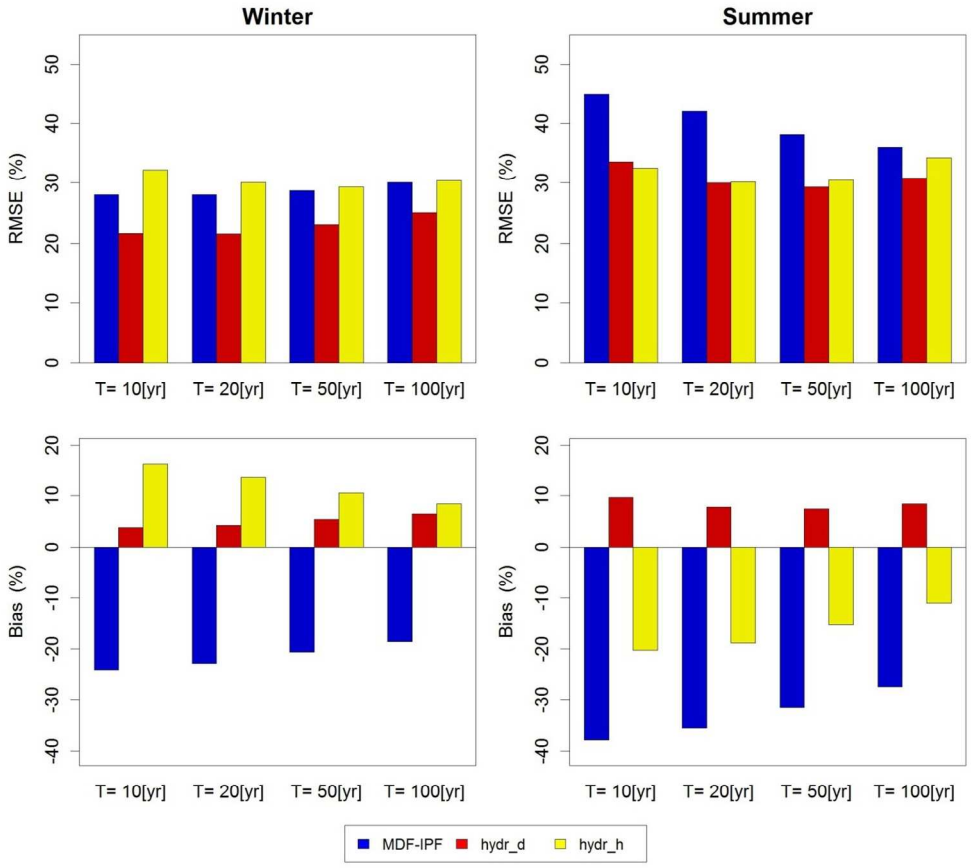

Figure 17. Comparison of the root mean square error (RMSE) and the bias using the hydr_d and hydr_h strategies for summer and winter seasons
165x150mm (220 x 220 DPI)